

Engineering Notes

Gravity-Induced Wrinkling in Subscale, Singly Curved Parabolic Gossamer Membrane

Jack Leifer*

Trinity University, San Antonio, Texas 78212
and

David C. Jones† and Adam M. Cook‡

University of Kentucky, Paducah, Kentucky 42002-7380

DOI: 10.2514/1.45672

I. Introduction

AS GOSSAMER structures are planned for possible deployment on various missions over the next decade, the development of verified computational models to predict their dynamic behavior on orbit is vital. This is because extensive testing of full-scale gossamer prototypes under operational conditions (e.g., 0 g, vacuum) is not possible on Earth due to their large size, and so computational models will be the primary means of exploring various design alternatives. To verify the accuracy of these computational models, subscale, full-field surface data from dynamic measurements of gossamer structures performed under various conditions (atmospheric and gravitational) will be used to verify subscale computational models, which can then be scaled up to predict full-scale structure performance. To increase the robustness of the subscale computational models, data for model verification need to be obtained under a variety of operating conditions. Whereas atmospheric loading of gossamer subscale models is typically varied by performing experiments in a vacuum chamber at various pressures, few (if any) experiments that specifically vary gravity field magnitude have been documented. The work presented here is a follow-up experiment to that performed by Meyer et al. [1] and contains new results from tests performed aboard NASA's KC-135A microgravity airplane, during which the surface contour of a singly curved parabolic membrane was measured at approximately 0, 1, and 1.8 g. The measurements were performed using close-range photogrammetry, a noncontact, full-field technique commonly used for the measurement of gossamer-class test articles [2,3]. Information pertaining to surface contour shape was extracted via photogrammetric analysis of simultaneous images of the membrane triggered during various times during the flight.

Presented as Paper 1833 at the 48th AIAA/ASME/ASCE/AHS/ASC Conference on Structures, Structural Dynamics and Materials: Gossamer Structures Forum, Honolulu, HI, 23–26 April 2007; received 27 May 2009; accepted for publication 3 November 2009. Copyright © 2009 by Jack Leifer. Published by the American Institute of Aeronautics and Astronautics, Inc., with permission. Copies of this paper may be made for personal or internal use, on condition that the copier pay the \$10.00 per-copy fee to the Copyright Clearance Center, Inc., 222 Rosewood Drive, Danvers, MA 01923; include the code 0022-4650/10 and \$10.00 in correspondence with the CCC.

*Associate Professor, Department of Engineering Science, One Trinity Place. Member AIAA.

†Undergraduate Assistant, Department of Mechanical Engineering; currently Structural and Space Systems Engineer, Redefine Technologies, Inc., Golden, Colorado.

‡Undergraduate Assistant, Department of Mechanical Engineering; currently Forensic and Design Engineer, Engineering Partners International—Material Testing Group, The Woodlands, Texas.

II. Background

The test article geometry chosen for this series of experiments corresponds to a one-half scale model of the PR-2 precipitation radar antenna reflector under joint development by the Jet Propulsion Laboratory (JPL) in Pasadena, California, and ILC Dover in Frederica, Delaware [4,5]. The scaled test article geometry was truncated to fit within the confines of the $1.524 \times 1.524 \times 0.914$ m³ enclosure designed to fly aboard NASA's KC-135A Microgravity Airplane. The KC-135A (since retired and replaced by a DC-9) on which the experiment flew was capable of generating short periods of approximately 0 g interspersed with 1 and 1.8 g conditions by following a repeated parabolic trajectory. A fixture, designed by JPL, used cork-lined parabolic clamps to maintain the edges of the membrane in the desired profile. Tension in the membrane was maintained by a set of cantilevered flexors mounted between one set of clamps and the fixed test frame. The precise angle and tension of the suspended clamp was controlled by manipulating set screws that contacted the membrane clamp, and the clamp's orientation with respect to the fixed frame was determined based on dial-gauge readings (Fig. 1).

III. Experimental Approach

For the current series of tests, a 76.2 μ m aluminized polyimide (Kapton® HN) membrane was installed in the test fixture and evaluated onboard the KC-135A at 0, 1, and 1.8 g (Fig. 1). The membrane contained about 5000 dots of 5 mm in diameter, which were uniformly silk-screened on approximately 12.5 mm centers over the entire membrane surface area (Fig. 2). These dots served as the targets on which the photogrammetric triangulation calculations were performed to obtain three-dimensional location information. This particular target density was chosen to allow surface wrinkle wavelengths (and other features) as small as 25 mm to be resolved. Six digital images were simultaneously triggered for each condition studied, with five used for the surface reconstruction (Fig. 2). The sixth image, taken by camera 1, documented the membrane clamp gauge readings, as well as the current acceleration state aboard the KC-135A, and allowed easy correlation of each set of digital images to membrane conditions (applied tension and gravity). The position of the membrane support clamps was changed gradually during the flight to tighten the membrane using the thumbscrew knobs located on the left side of the apparatus shown in Fig. 1. This work concentrates on the analysis of nine sets of images, each corresponding to one of two dial-gauge settings (one relatively slack, and one more taut) taken at three different local gravitational conditions in the order listed (Table 1).

The membrane contour moved (changed surface configuration due to gravitational acceleration change) between all image sets, with the exception of sets 4 and 5 (which were taken consecutively during a single pullout maneuver). Set 2 was taken at 1 g conditions while in level flight, before the beginning of the parabolic maneuvers. A comparison of image sets taken at identical conditions (sets 4, 5, and 7; sets 3 and 6) allows an evaluation of how stable and repeatable the membrane surface contour is as local gravitational conditions fluctuate during the flight. Because of the limited space within the test enclosure, the area of the reconstruction was 0.7×0.9 m², less than the full extent of the membrane surface.

IV. Image Processing Using Photogrammetry

A. Image Marking

For each set of five images used, image processing first required marking all target centroids visible in each view of the membrane. For the automated marking scheme to function correctly within the

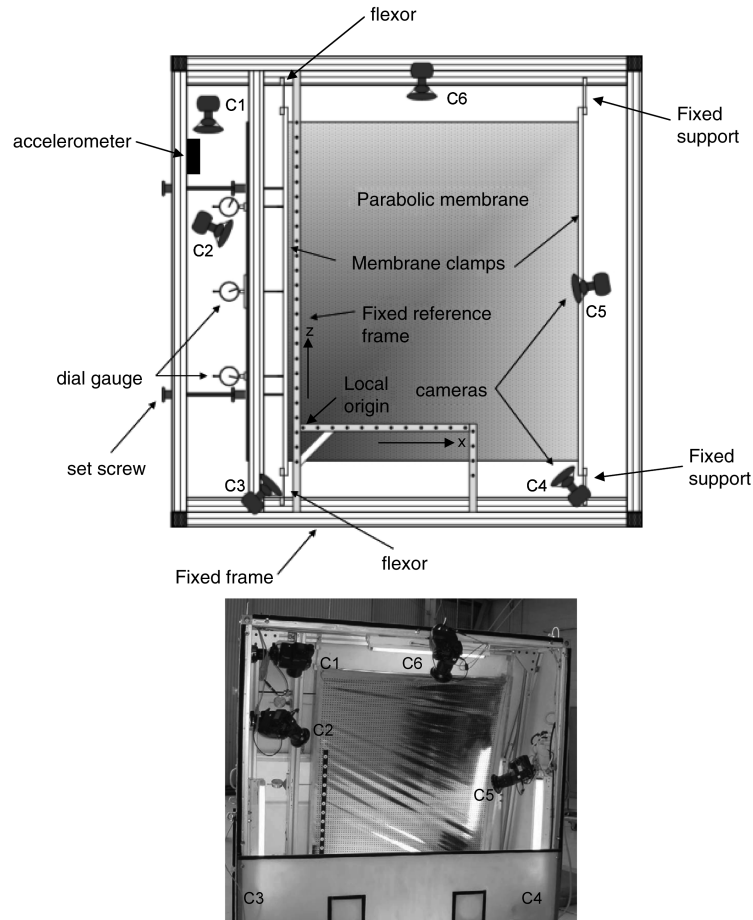


Fig. 1 Membrane tensioning and clamp positioning system: a) schematic diagram, and b) photograph. Cameras are demarcated at locations C1–C6. Cameras 3 and 4 (C3 and C4) in Fig. 1b are shielded from view by the opaque material affixed to the front-bottom portion of the enclosure.

software (PhotoModeler Pro v 5.2.3, Eos Systems, Inc., Vancouver, British Columbia, Canada), sufficient contrast between each target and the background must be present, the illumination across the specified region must be fairly even, and the target size must be relatively uniform. Examination of the problem areas extracted from the sample images (Fig. 2, regions A–D) shows that these requirements were not met over significant regions of the membrane studied here. These originated from the following:

- 1) The background of the membrane is mirror smooth and, therefore, contained reflected images that reduced the contrast between the targets and the background within the affected regions (A). In wrinkled regions, some multiple reflections were generated (B).

- 2) The target diameter-to-pixel ratio varied dramatically across each image, depending on each camera's position relative to the membrane (C, D). The target diameter-to-pixel ratios trended lower toward the bottom-left side of the membrane. Smaller ratios generally allow target centroids to be located with more precision.

Although the automated targeting tool provided by the software worked over large areas of each image, manual marking had to be used in regions affected by the above factors.

B. Target Referencing and Scaling

Once each of the visible membrane targets was marked in each image, corresponding targets within each photograph in the set had to be linked together, in a process called referencing. In applications such as this, in which many (virtually identical) target features are to be referenced, it is helpful to disperse a number of unique marks or patterns across the membrane surface, to provide visual cues for both location and direction [6]. The colored dot patterns (indicated in Fig. 2) distributed over the membrane surface were used in this case and were chosen specifically so that they could serve as both membrane targets and registration patterns. These were very helpful

during the fully manual referencing necessitated by the high target density and nonideal camera positions.

Scaling the three-dimensional surface reconstruction required the establishment of a membrane coordinate system for which the position did not vary with changes in gravity. A reference frame fabricated from aluminum (Fig. 2) was designed to fit within the experimental enclosure, in front of the membrane. Contrasting targets were attached to the horizontal and vertical members at approximately 2 in. (0.0508 m) intervals, and the system origin was defined to be the left-most target attached to the horizontal axis. These targets were marked and referenced along with those located on the membrane and provided the required fixed coordinate system.

V. Results and Discussion

A. Comparison of Reconstructed Membrane Contours

All image sets were processed using the procedures described in the previous sections, and contour surface plots of each reconstruction are shown in Fig. 3. The wire-frame grids shown in each figure reflect the gravity-induced changes in surface contour of the bottom two-thirds of the membrane and also show the effect of tension. They were generated via a commercial software package (Surfer v 8.04, Golden Software, Golden, Colorado), which used a Kriging algorithm to fit a surface to the three-dimensional *point cloud* (image reconstructions) generated by the photogrammetry software. The same point located on the fixed reference coordinate system was used as the origin of each plot.

Qualitatively, it is apparent that the edge tension is the most influential factor governing membrane surface contour. The relatively slack membrane conditions all possess wrinkles across the entire reconstructed membrane surface. The lower three plots, in contrast, show that increasing the tautness of the membrane significantly reduces (but does not eliminate) the surface wrinkling.

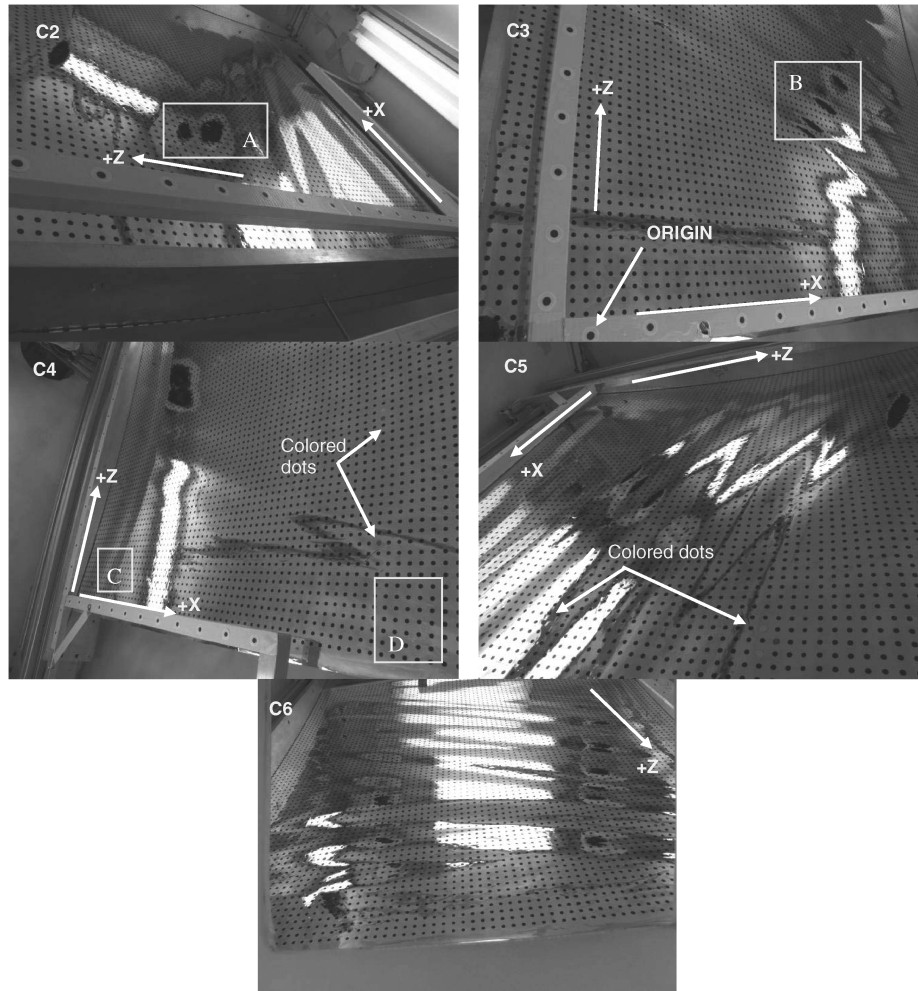


Fig. 2 Fields of view visible through each camera (C2–C6). Each of the images shown here were triggered simultaneously at 1 *g*. Top of the membrane is located in the +*Z* direction as shown on each image. The fixed circular targets on the aluminum frame were used as coordinate references; the +*X* and +*Z* directions are indicated. In addition, colored dots (as demarcated in images 4 and 5) were used on the membrane to assist with target referencing during the photogrammetric analysis. Note the reflected image of camera bootie (C2, region A), the multiple reflected images of one lens caused by wrinkling (C3 region B), and the change in apparent size of 5 mm targets across a single image (C4 regions C and D).

Although gravitational effects are clearly present, it is difficult to assess them quantitatively using the three-dimensional wire-frame reconstruction.

To quantitatively evaluate change in membrane contour as a function of gravity, the three-dimensional target locations computed by the photogrammetry software for each set of images were exported to standard spreadsheet software. “Columns” of targets, each representing a slice through the membrane were identified, and their *y* versus *z* coordinates were plotted for each set of images analyzed. These data are shown in Fig. 4 and depict “slices” through the membrane contour at *x* values corresponding to approximately $-0.06, 0.0, 0.2, 0.4, 0.6, 0.8$, and 0.9 m. These slices extended across the membrane parallel to the *z* axis, from the left membrane clamp

(located to the left of $x = -0.06$ m) to the right membrane clamp (located to the right of $x = 0.9$ m). A number of observations have been made through careful examination of these plots:

1) The targets located at approximately $x = -0.06$ reside along two curves that are both quite smooth and very similar in profile (though not identical) to both each other and to the parabolic clamps. The upper curve corresponds to the slack membrane, whereas the lower contour corresponds to the more taut condition. The similarity between the contour shapes is not unexpected, as this set of targets was located adjacent to the clamped portion of the membrane.

2) The targets located along the membrane at approximately $x = 0.9$ m were also expected to lie along a parabolic profile, because they were located adjacent to the right membrane clamp.

Table 1 Data sets analyzed in this study

Image set number	Gravitational acceleration, <i>g</i>	Dial-gauge setting (top/middle/lower)
2	1	25/25/25 mil (0.001/0.001/0.001 m)
3	0	25/25/25 mil (0.001/0.001/0.001 m)
4	1.8	25/25/25 mil (0.001/0.001/0.001 m)
5	1.8	25/25/25 mil (0.001/0.001/0.001 m)
6	0	25/25/25 mil (0.001/0.001/0.001 m)
7	1.8	25/25/25 mil (0.001/0.001/0.001 m)
35	0	220/190/165 mil (0.00855/0.00748/0.00650 m)
36	1.8	220/190/165 mil (0.00855/0.00748/0.00650 m)
37	1	220/190/165 mil (0.00855/0.00748/0.00650 m)

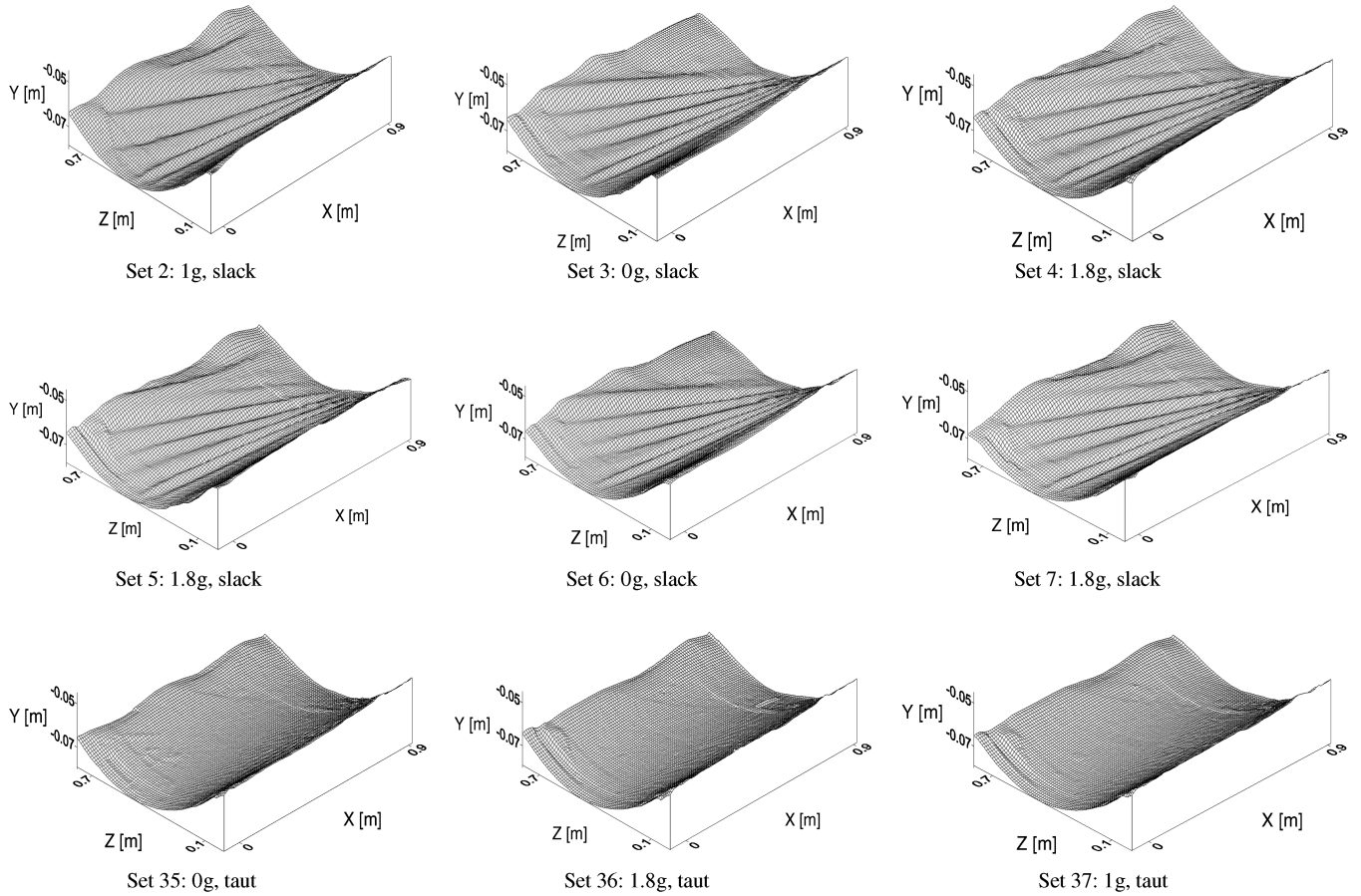


Fig. 3 Wire-frame surface contours of membrane generated through photogrammetric reconstruction.

Although there is some scatter in the data, it is apparent that the target locations did, in fact, follow a parabolic curve. As in the case of the targets located along the left membrane clamp, those associated with the taut condition fell along the bottom of the contour. Note that the gap in the plot extending approximately from $z = 0.3$ to 0.4 m was caused by a number of targets that were not within the fields of view of at least two cameras.

3) For the taut condition, the 0 g target locations (set 35) tended to float above those recorded for either the 1 g (set 37) or 1.8 g (set 36) target locations. This is true of all membrane contour slices extending from $x = 0$ through 0.9 .

4) For the slack condition, the 0 g (sets 3 and 6) and the 1.8 g (sets 4, 5, and 7) contours are each almost entirely superimposed. This effect is most apparent on the contour slices corresponding to $x = 0.2, 0.4$, and 0.6 . This superimposition provides more evidence that, after each resumption of a particular ambient gravitational condition aboard the aircraft, the membrane surface condition (e.g., wrinkle location, sag) can be recovered.

5) The parabolic shape imposed by the clamps on either side of the membrane did not extend across the entire surface of the membrane (along the x direction). Instead, the data show that the parabolic contour “flattened” (moved toward the intended focus) by about 4 mm in the central portion of the membrane (halfway between the clamps) for the taut case, and between 4 and 8 mm for the slack case. These measurements show that both wrinkling and flattening can be reduced by tightening the membrane.

B. Estimate of Accuracy

Because each set of images was scaled using the same set of coordinate system points, the variation in locations computed in each of the three-dimensional reconstructions for each target affixed to the fixed struts can be used to provide an indication of baseline measurement resolution. These have been calculated and are shown in Table 2. In the labeling scheme used, H1 indicates the first point on

the horizontal strut to the right of the origin; V1 indicates the first point on the vertical strut located above and slightly left of the defined origin point. Only points for which the locations were determined in at least four images in each set analyzed were included in the table. Clearly, measurement precision decreased abruptly around the upper end of the vertical coordinate axis, as indicated by the increased standard deviation values. These data also show that measurement precision generally deteriorates with absolute distance from the origin $(0,0,0)$ point and is the likely cause of the increase in scatter as both x and z increase.

Table 2 Variation in coordinate point locations measured relative to the system origin and their standard deviations (nine measurements at each position were used to compute the mean)

Point	Mean position, m	Standard deviation, m
V1	0.04383	2.832e-5
V2	0.08473	6.7182e-5
V3	0.1345	9.4486e-5
V4	0.1858	1.2694e-4
V5	0.2312	1.5179e-4
V6	0.2814	2.1113e-4
V7	0.3334	2.0475e-4
V8	0.3827	2.0956e-4
V9	0.4306	2.6771e-3
V10	0.4829	3.1119e-3
V11	0.5347	3.2915e-3
H1	0.1504	6.208e-5
H2	0.2024	6.441e-5
H3	0.253	7.362e-5
H4	0.3038	1.224e-4
H5	0.3552	8.988e-5
H6	0.4057	1.502e-4
H7	0.4568	1.663e-4

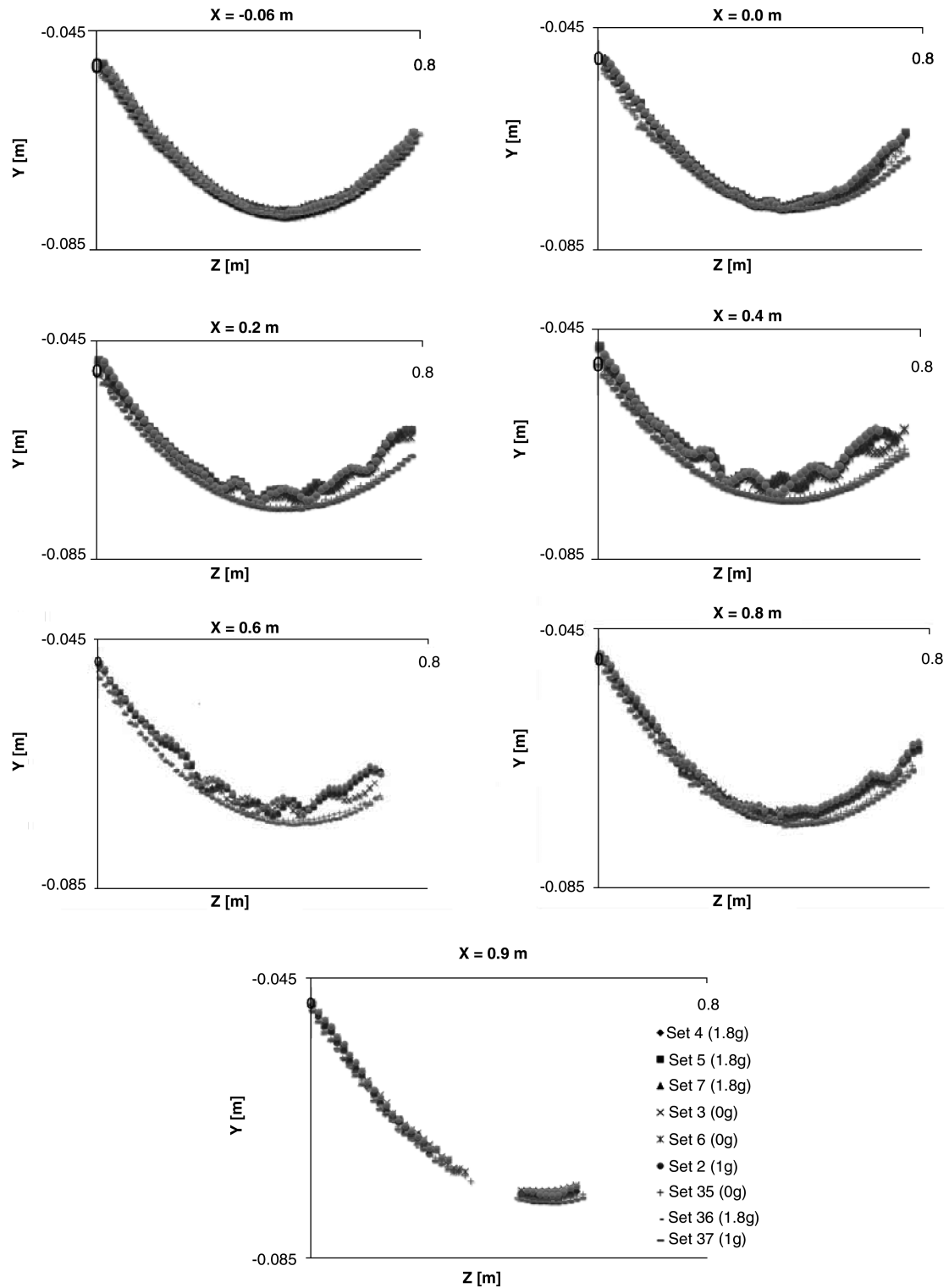


Fig. 4 Membrane contour slices.

VI. Conclusions

In this study, photogrammetry was used to reconstruct the three-dimensional surface contour of a parabolic membrane as a function of local gravity vector, which varied due to the parabolic trajectory flown by NASA's KC-135A. From a visual inspection of the wire-frame membrane contours corresponding to the slack condition at 0 and 1.8 g, the apparent similarities among the surface configurations at each respective local gravity condition indicate that the equilibrium membrane surface shape attained at a particular set of conditions can be substantially recovered, even after intermediate periods of changing local gravity conditions. The quantitative analysis of the

membrane contour data supports this conclusion. At increased tension levels, the wrinkles in the membrane smoothed out and the contour sag level remained virtually constant as a function of changing local gravity conditions.

Acknowledgments

Funding for the experimental portion of this work was provided by the Kentucky Space Grant Consortium, the University of Kentucky Executive Vice President for Research, and the University of Kentucky College of Engineering. The experimental measurements

aboard the KC-135A were performed through the NASA Reduced Gravity Student Flight Opportunities Program. The authors gratefully acknowledge the participation of flight crew members Britton Wainscott, Chris Thompson, and Ben Morgan, as well as team member Justin Hastie, who all participated while undergraduates at the University of Kentucky/Extended Campus Program at Paducah. Invaluable technical advice pertaining to the experimental work was provided by Chris Meyer, then of Swales Aerospace, and Bernardo C. Lopez, of the Jet Propulsion Laboratory. Support of the first author for overseeing the image data reduction was provided through the Tom and Mary Turner Junior Faculty Fellowship for Summer Research at Trinity University. Some photo sets presented herein were processed by Matthew Saunders, a Trinity University undergraduate, as well as Raymond Aguilar and Vivian Parades, high school students who participated in this project through Trinity University's Upward Bound Program.

References

- [1] Meyer, C. G., Leifer, J., Lopez, B. C., Jones, D. C., and Caddell, B. C., "Zero- and One-g Comparison of Surface Profile in Single-Curved Parabolic Membrane," *Journal of Spacecraft and Rockets*, Vol. 42, No. 6, Nov. 2005, pp. 1101–1108; also AIAA Paper 2004-1736, April 2004.
- [2] Pappa, R. S., Giersch, L. R., and Quagliaroli, J. M., "Photogrammetry of a 5 m Inflatable Space Antenna with Consumer Digital Cameras," NASA TM-2000-210627, 2001.
- [3] Pappa, R. S., et al., "Photogrammetry Methodology Development for Gossamer Spacecraft Structures," AIAA Paper 2002-1375, 2002.
- [4] Im, E., Durden, S. L., Kakar, R. K., Kummerow, C. D., and Smith, E. A., "The Next Generation of Spaceborne Rain Radars: Science Rationales and Technology Status," *SPIE's Third Symposium on Microwave Remote Sensing of the Atmosphere and Environment*, Society of Photo-Optical Instrumentation Engineers, Bellingham, WA, Oct. 2002, pp. 10–02.
- [5] Lin, J. K., Sapna, G. H. III, Scarborough, S. E., and Lopez, B. C., "Advanced Precipitation Radar Antenna Singly Curved Parabolic Antenna Reflector Development," *4th Gossamer Spacecraft Forum, 44th AIAA SDM Conference*, AIAA, Reston, VA, 2003, pp. 4–03; also AIAA Paper 2003-1651.
- [6] Pappa, R. S., Jones, T. W., Black, J. T., et al., "Photogrammetry Methodology Development for Gossamer Spacecraft Structures," AIAA Paper 2002-1375, April 2002.

G. Agnes
Associate Editor